

**PHOTOCATALYTIC DEGRADATION OF
RHODAMINE B USING AG/AGCl@GO**

**A Thesis Submitted to
the Graduate School of Engineering and Sciences of
İzmir Institute of Technology
in Partial Fulfillment of the Requirements for the Degree of
MASTER OF SCIENCE
in Chemical Engineering**

**by
Taylan Can KÖSE**

**March 2023
İZMİR**

ACKNOWLEDGEMENTS

I would like to acknowledge and give my warmest thanks to my advisor, Prof. Dr. Fehime ÖZKAN who made this study possible. Her guidance, advice and support carried me through all the stages of my M.Sc. Thesis.

I would like to thank to Assoc. Prof. Dr. Aslı Yüksel ÖZŞEN, Gizem SAYGI for their assistance and support during this study.

I am also grateful to my friends Pelin KELEŞ, Özgür Enes TAYTAŞ, Emre DEĞİRMENCİ, Emre DEMİRKAYA, Gözde GÖZEL, Damla YALÇIN, Nilay POLAT for their support, friendships, assistance to my work.

I would like to thank İzmir Institute of Technology Center For Materials Research for providing technical support and help.

Finally, I express my sincere thanks to my family Birol KÖSE, Hatice KÖSE, and Sıla Naz KÖSE for their love, support, encouragement and patience throughout my education.

ABSTRACT

PHOTOCATALYTIC DEGRADATION OF RHODAMINE B USING AG/AGCl@GO

Water is an essential source for earth. According to the United Nation's report, every day 1800 children dies because of contaminated water. Dyes are one of the most common water pollutants. They are using in many areas like cosmetic, textile, pharmaceutical etc. Every year nearly 140,000 tons of dye releasing to the environment. Therefore, removal of dyes from water is an essential topic. There are many ways to remove dyes from water. However, studies showed that traditional methods are ineffective to removing pollutants from water. On the other hand, photocatalysis is a promising technology.

In this study, Ag/AgCl and Ag/AgCl@GO photocatalysts were synthesized and their removal performances on Rhodamine B dye were investigated. In addition, the parameters affecting the removal performance were also studied.

Characterization tests such as synthesized photocatalysts, XRD, BET, UV-Vis Analysis, TGA, SEM, TEM was carried out. According to the XRD results, the peak regions of the synthesized photocatalysts were similar to other studies in the literature. The synthesized photocatalysts were first studied under 3 different pH values (pH:3, pH:8, pH:11) using 10 ppm rhodamine b dye and 30 mg catalyst under UV light. According to the results, for both photocatalysts, their natural pH, namely pH:8, showed the best performance. Afterwards, experiments were carried out with different photocatalyst weights and it was observed that the removal performance did not change after 40 mg. Finally, different dye amounts were studied and it was observed that as the dye amount increased, its removal decreased. It has been observed that the addition of graphene oxide significantly improves the performance of the catalyst.

ÖZET

AG/AGCl@GO KULLANARAK RODAMİN B'NİN FOTOKATALİTİK BOZUNMASI

Su, gezegenimiz için vazgeçilmez bir kaynaktır. Birleşmiş Milletler'in raporuna göre her gün 1800 çocuk kirli su nedeniyle ölüyor. Boyalar en yaygın su kirleticilerinden biridir. Kozmetik, tekstil, ilaç vb. birçok alanda kullanılmaktadırlar. Her yıl yaklaşık 140.000-ton boya çevreye salınmaktadır. Bu nedenle boyaların sudan giderimi önemli bir konudur. Boyaları sudan gidermenin birçok yolu vardır. Ancak araştırmalar, geleneksel yöntemlerin kirleticileri sudan uzaklaştırmada etkisinin düşük olduğunu göstermiştir. Öte yandan, fotokataliz gelecek vaat eden bir teknolojidir.

Bu çalışmada Ag/AgCl ve Ag/AgCl@GO fotokatalizörleri sentezlenmiş ve Rhodamine B boyası üzerindeki giderim performansları incelenmiştir. Ayrıca giderim performansına etki eden parametreler de incelenmiştir.

Sentezlenen fotokatalizörler, XRD, BET, UV-Vis Analizi, TGA, SEM, TEM gibi karakterizasyon testleri yapılmıştır. XRD sonuçlarına göre sentezlenen fotokatalizörlerin pik bölgeleri literatürdeki diğer çalışmalarla benzerlik göstermiştir. Sentezlenen fotokatalizörler önce 3 farklı pH değerinde (pH:3, pH:8, pH:11) 10 ppm rodamin b boyası ve 30 mg katalizör kullanılarak UV ışığı altında çalışıldı. Sonuçlara göre her iki fotokatalizör için de doğal pH'ları yani pH:8 en iyi performansı göstermiştir. Daha sonra farklı fotokatalizör ağırlıkları ile deneyler yapılmış ve 40 mg sonrasında giderim performansının değişmediği gözlenmiştir. Son olarak farklı boya miktarları çalışılmış ve boya miktarı arttıkça gideriminin azaldığı görülmüştür. Grafen oksit ilavesinin, katalizörün performansını önemli ölçüde iyileştirdiği gözlemlenmiştir.

TABLE OF CONTENTS

LIST OF FIGURES	vi
LIST OF TABLES	viii
CHAPTER 1: INTRODUCTION	1
CHAPTER 2: LITERATURE SURVEY	5
2.1. Dyes and Water Pollution	5
2.2. Dyes and Classification of Dyes	5
2.4. Dye Removal Processes	13
2.5. Photocatalytic Degradation	17
CHAPTER 3: MATERIALS AND METHODS	20
3.1. Materials	20
3.2. Synthesis of Photocatalysts	20
3.3. Characterization Studies	24
3.4. Photocatalytic Experiments	25
CHAPTER 4: RESULTS AND DISCUSSIONS	27
4.1. Characterization Results of Ag/AgCl and Ag/AgCl@GO Photocatalysts	27
4.2. Photocatalytic Degradation Results of RhB	30
CHAPTER 5: CONCLUSION	39
REFERENCES	40

LIST OF FIGURES

<u>Figure</u>	<u>Page</u>
Figure 1.1. Classification of dyes	2
Figure 1.2. Number of scientific studies in literature about dye removal	3
Figure 2.1. The schematic diagram of photo-degradation mechanism	19
Figure 3.1 Synthesis diagram of Ag/AgCl@GO photocatalyst	21
Figure 3.2 Silver nitrate solution (a), Solution with added GO (b), Solution after adding KCl (c,d), Final product Ag/AgCl@GO (e)	21
Figure 3.3. Synthesis diagram of Ag/AgCl photocatalyst	22
Figure 3.4. Silver nitrate solution (a), Solution after adding KCl (b), Final product Ag/AgCl (c)	23
Figure 3.5. Synthesis diagram of UiO-66-NH ₂	23
Figure 3.6. Synthesis diagram of UiO-66-NH ₂ -Ag/AgCl	24
Figure 3.7. Chemical structure of rhodamine B dye (Source: Alé et al. 2020)	25
Figure 3.8. Experimental setup	26
Figure 3.9. The emission spectra of RhB in different concentrations	26
Figure 4.1. XRD of Ag/AgCl@GO and Ag/AgCl	28
Figure 4.2. SEM images and particle size graphs of Ag/AgCl@GO (a) Ag/AgCl (b), UiO-66-NH ₂ -Ag/AgCl (c)	29
Figure 4.3. TGA results of Ag/AgCl (a), Ag/AgCl@GO (b), and UiO-66-NH ₂ -Ag/AgCl (c)	30
Figure 4.4 Concentration change for different pH values with time	32

<u>Figure</u>	<u>Page</u>
Figure 4.5. Photocatalytic degradation performance of each photocatalysts for different catalyst amounts (at their neutral pH (8) values)	33
Figure 4.6. Concentration changes with time of each photocatalysts for different catalyst amounts (at their neutral pH values).....	34
Figure 4.7. Photocatalytic degradation performance of photocatalysts with different dye amount	35
Figure 4.8. RhB photodegradation without light	36
Figure 4.9. Comparison of concentration change of each samples with time.	36
Figure 4.10. Kinetic data of photocatalysts with pseudo-first-order- model.....	39

LIST OF TABLES

<u>Table</u>	<u>Page</u>
Table 2.1. Classification of dyes based on chemical structure	7
Table 2.2. Classification according to usage, examples, and toxic effects of dyes	10
Table 2.3. Properties of RhB dye	13
Table 4.1. PL results of samples	38

CHAPTER 1

INTRODUCTION

Water is an essential element for the earth and directly affects human life. 70% of the earth's surface is water, however reaching clean, drinkable water is still a problem, because of the contamination of water resources (Ahmad et al. 2021). The United Nations reports that every day 1800 children under age 5 dies because of contaminated water. Household, agricultural and industrial wastes making water non-usable (Chowdhury 2012).

Dyes are one of the most common water pollutants and using in many areas such as cosmetics, textiles, printing, food, paper, pharmaceutical, etc. (Sundararajan et al. 2017). Every year nearly 800,000 tons of dye produces and 140,000 tons of the are released into the environment (Slama et al. 2021).

There are two important components for dye molecules which are chromophores and auxochromes. Chromophores are the components that produce color. Auxochromes make the molecule water-soluble, giving it the ability to bind to fibers and complement the chromophore (Hunger 2003).

Dyes can classify in various ways. One of them is classifying dyes according to their solubility. Soluble dyes include anionic and cationic dyes. Insoluble dyes include non-ionic dyes (Rafiq et al. 2021). Figure 1.1 shows the classification of dyes according to their solubilities (Samsami et al. 2020).

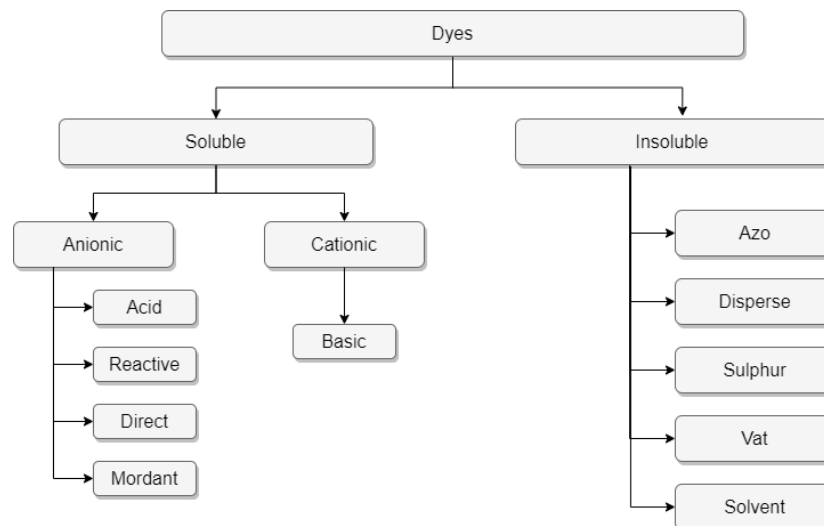


Figure 1.1. Classification of dyes.

Rhodamine B (RhB) is a widely used organic dye, synthetic, water-soluble, and carcinogenic. Due to its high stability and non-biodegradable, it is mainly used as a pigment in industries such as textile, paper, cosmetics, and leather. Wastewater contaminated with RhB can affect animals and humans with serious health problems. It is carcinogenic and neurotoxic even at very low concentrations. Therefore, the removal of RhB from water is a necessary topic to consider (Bhat et al. 2020).

Until the 2000s paint removal of dyes were not very important. Figure 1.2 shows the number of publications about dye removal. At the beginning some physical treatment methods were used such as sedimentation (Gupta et al. 2009). In today's world, coagulation/flocculation, electrocoagulation, Fenton, membrane filtration, ion-exchange, adsorption, and some hybrid methods such as filtration with coagulation methods are using frequently. However, even these methods are giving good results, they have some disadvantages (Piaskowski et al. 2018). For example, coagulation has sludge formation and removal of this sludge is one of the biggest disadvantages. Operating cost is another parameter to consider (Dutta et al. 2021).

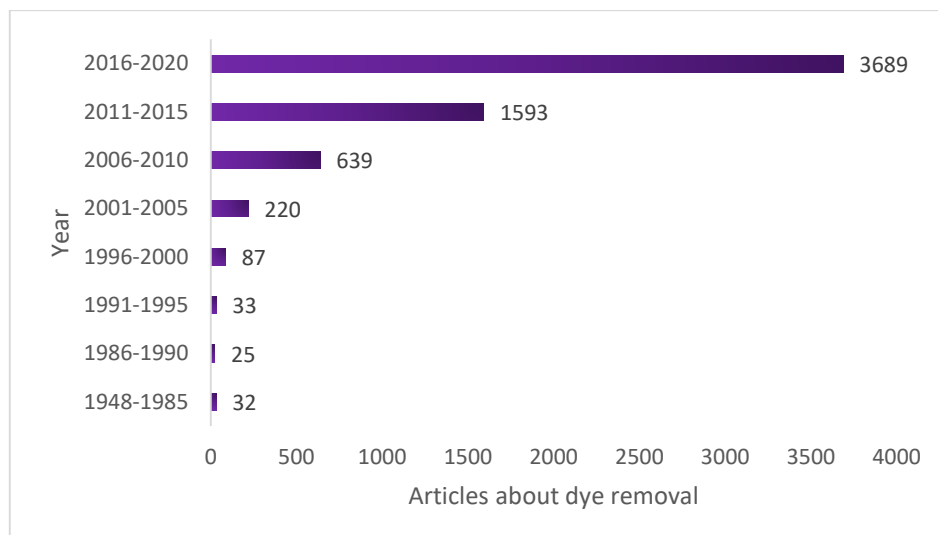


Figure 1.2. Number of scientific studies in literature about dye removal.

Photocatalysis degradation is a more preferable method because of its high efficiency, an environmentally friendly, cost-efficient method (Allé et al. 2020). Basically, in a dye degradation, smaller molecule (water, carbon dioxide, and other by-products) occurs from the oxidation of larger molecules. Essentially, an electron transfer occurs from the valance band to the conduction band onto the surface of a semiconductor while it is lightening with a suitable wavelength. The Hydroxide radicals and superoxide anion's reaction are produced with of generated with water or oxygen (Viswanathan 2018).

Silver is a material that has strong visible absorbance is used for many processes as elemental nanoparticle. There are many studies because of the semiconducting ability of silver halides. Silver/Silver halide composites are very suitable for photocatalytic studies because of its plasmon resonance in the visible region. To improve the performance of the photocatalyst is combining it with a functional material (Ai 2019).

Graphene Oxide (GO) is very suitable material to improve performance of Silver/Silver halide composites and photocatalysts because of its high stability, active surface chemistry and unique monolayer structure. It is also able to broad the absorption wavelength range and reduce to band gap of the composite material. In photocatalysts, GO also able to increase the surface area of the catalyst and adsorption performance of the catalyst (Ai 2019).

Metal-organic frameworks are a class of porous crystalline polymers composed of organic binders combined with metal ions. MOFs often have 3D frameworks, high surface area, adjustable pore size, and many other properties. By combining suitable

organic ligands with metal, MOFs can be combined in almost unlimited ways. MOFs can be imparted to certain chemical properties by in-situ synthesis or postsynthetic modification. Thanks to these advantages, MOFs can be used in areas such as adsorption, catalysis, gas storage, photocatalytic degradation (Zou et al. 2019).

UiO-66 is one of the most popular MOFs used in the literature. This MOF contains Zr and also has a structure that can absorb ultraviolet (UV) light due to its wide band gap, is water resistant and largely impervious to sunlight. This band gap energy can be slightly changed by the addition of the amino group. The photoabsorption edge of UiO-66-NH₂ shifts from the UV region to the visible light region. However, preventing the solar radiation of UiO-66-NH₂; There are factors such as insufficient light absorbability and short carrier life. Therefore, many schemes have been used, such as metal nanoparticle charging, semiconductor coupling, and organic binder/metal core decoration (Zhao et al. 2019).

In this study, Ag/AgCl, Ag/AgCl@GO, UiO-66-NH₂-Ag/AgCl composite catalysts were synthesized and characterized. The photocatalytic performance was calculated with remove efficiency from UV-Vis light results. Synthesis method, parameters that effect the degradation performance were also discussed in further chapters.

CHAPTER 2

LITERATURE SURVEY

2.1. Dyes and Water Pollution

Dye is a substance that has chemical bonding to the layers. They are usually applied as an aqueous solution (Steingruber 2004). The dye industry is growing rapidly which increases the effluent amount and that negatively affects living life. Every year, nearly 1,000,000 tons of dyes which are using in various industries such as textile, food, cosmetics, and pharmaceutical are producing in the world (Maheshwari et al 2021). According to the World Bank report, about 20% of water pollution is caused by the dying industry and textile finishes. Every year nearly 140,000 tons of these dyes are released into the environment. These effluent dyes are polluting water resources. Especially, in the textile industry, wastewater has a high concentration of dye (Rashid et al. 2020). In the textile industry, color is one of the most important factors for selling the product. Until the mid-1800s, only limited and dull colors were used in industry due to the use of natural dyes. Even after exposure to sunlight, discoloration was observed. To fix these problems, mordants were developed that bind fiber and dye together. In this way, wider and brighter color tones were achieved (Whitaker and Willock 1949). However, mordants can be very toxic and have negative effects on water sources. In the textile industry, while 80% of dyestuffs stay on the fabric, the rest binds water and forms wastewater (Kant 2011). According to Kant's study, there are 72 different toxic chemicals in the textile dying wastewater. Nearly 30 of these toxic chemicals cannot be removed (Kant 2011).

2.2. Dyes and Classification of Dyes


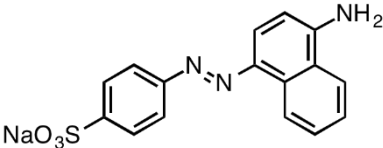
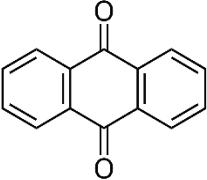
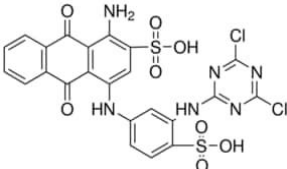
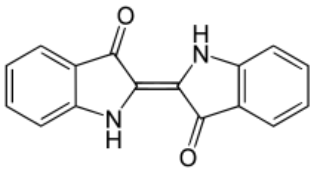
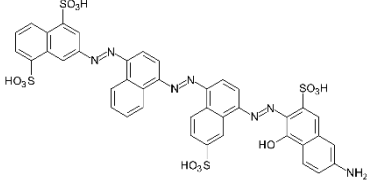

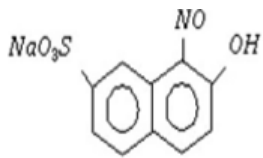
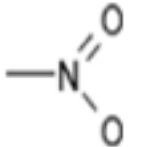
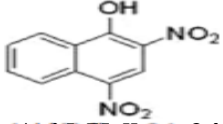
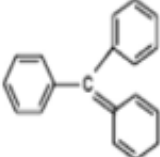
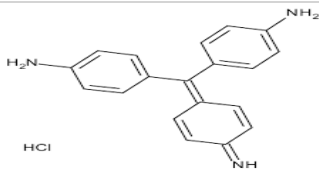
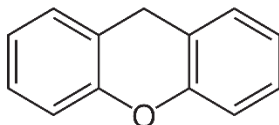
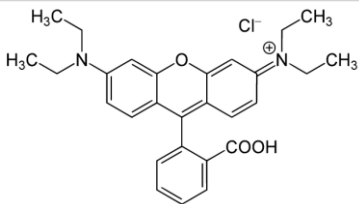
Dyes are organic compounds or mixtures that are using to colorize surfaces such as fabric, paper, and plastic. Unlike organic compounds, dyes consist of a chromophore group that absorbs light between the wavelengths of 400-800 nm in the visible spectrum, and auxochromes that reinforce the properties of this chromophore group. Chromophores are an unsaturated group responsible for the absorption of light in the UV or visible

region. Common examples of chromophores are azo (-N=N-), methyl (-CH=), nitro (-NO₂) and carbonyl (-C=O) groups. Chromogens are compounds with aromatic rings that contain a chromophore. Most dyes also contain groups called auxochromes, such as hydroxyl (-OH) and amine (-NH₃), which serve to intensify the color. A chromogen without an auxochrome group cannot act as a dye. Dyes can be classified in various ways, but mostly they may be classified according to their chemical structure and usage area (Gürses et al. 2016).

2.2.1. Chemical Classification

The chemical classification method has some advantages. For example, paints can be defined according to the group they belong to, according to their characteristics. Another advantage is that it is easier to manage since there are approximately 12 chemical groups. Table 2.1 summarizes the classification of dyes based on chemical structure.

Table 2.1. Classification of dyes based on chemical structure.

Class	Chromospheres	Example
Azo Dyes		 <p>Direct Brown 78</p>
Anthraquinone Dyes		 <p>Reactive Blue 4</p>
Indigoid Dyes		 <p>Acid Blue 71</p>
Nitroso Dyes		 <p>Acid Green 1</p>
Nitro Dyes		 <p>Acid Yellow 24</p>
Triarylmethane Dyes		 <p>Basic Red 9</p>
Xanthene Dyes		 <p>Rhodamine B</p>

2.2.1.1. Azo Dyes

Azo dyes are the dye types that have the largest share among synthetic dyes. High stability, high color density, ease of use, and versatility are the characteristics of azo dyes. They are usually attached to an aromatic aromatic ring or heterocyclic compound and are attached on the other side to an unsaturated carboxyl, sulfonyl, heterocycle, or aliphatic group. It has a certain chromophore structure (-N=N-), which makes the dye water-soluble and attaches to the fiber. According to the number of azo groups, they are divided into three classes: mono, di, and poly (Slama et al. 2021, Zhan et al. 2018).

2.2.1.2. Anthraquinone Dyes

Anthraquinone dyes are widely used in the textile dyeing industry. They are soluble in water and have sulfonic acid content. Their bright colors, durability, and excellent fastness are their most well-known characteristics (Slama et al. 2021, Shahid et al. 2019).

2.2.1.3. Indigoid Dyes

Indigo dyes are dyes based on the plant "Indigofera tinctoria" and are the oldest known dye type. They are insoluble in water but become soluble in water after alkali reduction. The textile dyeing process takes place in its water-soluble form. The water-soluble dye is oxidized by exposure to air and adhered to the fabric, while the dye returns to its keto form. Indigo dyes are used to color jeans (Slama et al. 2021).

2.2.1.4. Nitroso Dyes

Nitroso dyes are dyes that have an OH group and a nitroso group in the ortho position in the structure of this OH group. They are produced by the action of sodium nitrite on aromatic hydroxy compounds in an acid medium. It is resistant to light and heat effects. It is used in fields such as dyeing rubber, wallpaper, pencil production, the varnish industry, dyeing wool and silk, and coloring soap (Chekalin 1972).

2.2.1.5. Nitro Dyes

Nitro dyes are still used today due to their ease of production and high light durability. There is NO₂ radical in chromophore groups (Gürses et al. 2016).

2.2.1.6. Triarylmethane Dyes

Triphenylmethane dyes are water-soluble and have a wide color scale. Varieties containing sulfonic acid in auxochrome can be used as an indicator. It is generally used for dyeing wool and silk protein fibers because it consists of two groups of sulfonic acids (Slama et al. 2021, Ananthashankar et al. 2014).

2.2.1.7. Xanthene Dyes

Xanthene dyes are fluorescent dyes that can have acid or basic characteristics. Xanthene dyes are grouped as diphenylmethane, triphenylmethane, amino hydroxy, and fluorescent derivatives. Paper can be used in various industrial fields such as paint, medicine, ink, and textile. Fluorescence properties are the main motivation for use (Slama et al. 2021).

2.2.2. Usage Classification

Usage or application classification is a system based on the Colour Index. The advantage of this system is to consider the classification according to the use or application method before considering the structure and other detailed information of the dye (Hunger 2003). Usage or application classification is briefly explained in Table 2.2.

Table 2.2. Classification according to usage, examples, and toxic effects of dyes (Sources: Gupta 2008, Hunger 2003).

Class	Usage Area	Example	Toxic Effects
Cationic (Basic) Dye	Paper, polyacrylonitrile, modified nylons, modified polyesters	Rhodamine B, Methylene Blue	Changes physical and chemical properties of water, Harms plant life and wild life
Acid Dye	Textile, nylon, wood, silk, leather, cosmetics, modified acrylics, food	Acid Orange, Acid Blue	Carcinogenic, Vomiting, Diarrhea
Disperse Dye	Polyester, nylon, cellulose, acetate, acrylic fibers	Disperse Red 9, Disperse Violet 1	Carcinogenic, Soil and water pollution
Direct Dye	Dyeing cotton and rayon, paper, leather and nylon	Congo Red, Direct Black 38	Carcinogenic, Dermatitis, Damages aquatic animals and plants
Vat Dye	Cellulosic fibers, wool, natural fibers	Vat Blue 1	Allergic, Dermatitis, Rhinitis, Reduces quality of water
Reactive Dyes	Cotton, silk, wool, nylon	C.I. Reactive Blue 19, C.I. Reactive Red 120	Allergic reactions Dissolved solids in effluent
Solvent Dyes	Plastic, gasoline, oils, lubricants, waxes	Solvent Red 24, Solvent Yellow 33	Harms aquatic life, Dermatitis, Breathing problems
Sulfur Dyes	Cotton, rayon, wood, paper, silk, leather, polyamide fibers	Sulfur Brilliant Green, Sulfur Black 1	Skin damage, itchy, blocked nose, carcinogenic
Reactive Dyes	Cotton, silk, wool, nylon	C.I. Reactive Blue 19, C.I. Reactive Red 120	Allergic reactions Dissolved solids in effluent
Solvent Dyes	Plastic, gasoline, oils, lubricants, waxes	Solvent Red 24, Solvent Yellow 33	Harms aquatic life, Dermatitis, Breathing problems
Sulfur Dyes	Cotton, rayon, wood, paper, silk, leather, polyamide fibers	Sulfur Brilliant Green, Sulfur Black 1	Skin damage, itchy, blocked nose, carcinogenic

2.2.2.1. Cationic (Basic) Dyes

Cationic dyes are dyes that convert anionic fiber textiles into colored cationic salts. They are sensitive to light. They are used for dyeing paper, nylon, and modified polyesters. The main chemical classes of these dyes are cyanine, triarylmethane, anthraquinone, diarylmethane, diazahemicyanin, oxazine, hemicyanin, thiazine and hemocyanin (Gupta 2008, Slama et al. 2021).

2.2.2.2. Acid Dye

Acid dyes are water-soluble and low-pH dyes that have acidic groups such as SO₃H and COOH in their structures. They are often used to dye wool. However, some acid dyes are used as food colorants and some are also used to dye organelles in the medicine area (Booth, Gerald 2000, Hunger 2003).

2.2.2.3. Disperse Dye

Disperse dyes are the smallest molecules of dyes. They are insoluble in water and are stable only at high temperatures (Slama et al. 2021).

2.2.2.4. Direct Dye

Direct dyes are a type of dye known for their affordable cost. They are soluble in water. They combine with inorganic electrolytes and anionic salts such as sodium sulfate or sodium chloride to have a high bonding ability for cellulosic fibers. Therefore, when washing, they should be washed in a cold cycle and with fabrics of their color (Gupta 2008, Slama et al. 2021).

2.2.2.5. Vat Dye

They are dyes containing anthraquinone and indigoides in their structure. They are insoluble in water. They must be reduced to be water-soluble and therefore used with reducing agents such as sodium hyposulfite. Since its use requires complex operations, their use is gradually decreasing (Gupta 2008, Gürses 2016).

2.2.2.6. Reactive Dye

Reactive dyes work well with cellulosic and some protein fibers. They are water-soluble dyes. They are versatile dyes due to their permanent effects, their ability to work in a wide temperature range, their easy manipulation, and their high pigmentation. At the same time, they can form covalent bonds with multiple fibers due to some reactive groups they contain. They have a simple chemical structure and their absorption bands are narrow (Gupta 2008, Gürses 2016, Slama et al. 2021).

2.2.2.7. Solvent Dye

They are solvent-soluble dyes and are insoluble in water. Their structure is generally non-polar, which leaves them without polar solubilizing groups such as sulfonic acid and carboxylic acid. It is used in fields such as plastic, gasoline, lubricant, oils and waxes (Gupta 2008).

2.2.2.8. Sulfur Dye

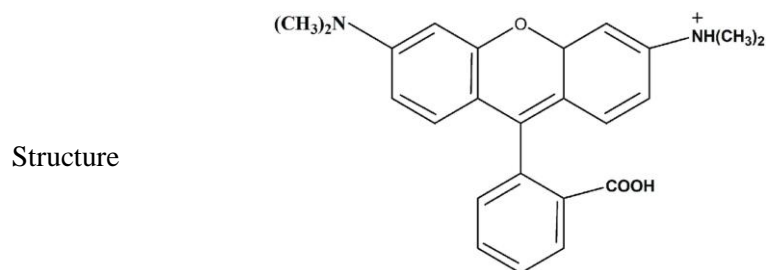
Sulfur dyes are economically important dyes as they have improved dyeing properties, easy usability, low cost, and good washing fastness. They have limited use. It is generally used in the fields of silk, leather, paper, wood, cotton, and rayon (Gupta 2008, Slama et al. 2021).

2.3. Rhodamine B

Rhodamine B (RhB, [Table 2.3](#)) is one of the most widely used dyes in the industry. It is used as a colorant in the textile industry due to its high stability and non-biodegradable which makes it a xanthene class dye (Al-Gheethi et al. 2022).

Table 2.3. Properties of RhB dye.

Molecular Formula	$C_{28}H_{31}ClN_2O_3$
C.I. Name	Basic Violet 10
CAS Number	81-88-9
Molecular Weight	
(g/mol)	479
λ_{max} (nm)	554
Solubility	5 mg in 100 mL



RhB, a carcinogenic and neurotoxic dye, causes developmental and reproductive problems in humans and animals and also causes skin, respiratory and gastrointestinal irritation. In addition, it causes cough, shortness of breath, wheezing, vomiting, nausea, headache, chest pain, and even worse, it has the possibility of forming tumors. It is toxic when exposed even in very small amounts and causes death in high doses. Preventing the refraction of light causes a decrease in photosynthesis, which endanger aquatic life. Zooplankton and phytoplankton are less common in RhB-contaminated waters (Imam et al. 2020)

2.4. Dye Removal Processes

Over the last decades, environmental impacts of the dyes were never considered. After the increase in production rate of dyes, their toxicity and nature become more remarkable. Therefore, removal of the dyes become an important topic in industry (Ajmal 2014). There was no effluent discharge limit. Therefore, the treatments were started with some traditional methods like sedimentation and equalization to adjust the total suspended solids (TSS), total dissolved solids (TDS) and pH of the water (Gupta 2008).

ETAD (Ecological and Toxicological Association of the Dyestuffs Manufacturing Industry) is an organization founded in 1974, they are working with governments and public officials to protect the environment, protect consumers and inform people about the harmful effects of products. After gaining awareness, some governments such as England and Scotland began to apply strict rules for the removal of dye from industrial wastewater. The European Community (EC) also has many strict rules on this subject. Turkey is among the countries that implement these rules (Samsami et al. 2020).

Removal of the dyes from wastewater was classified into 3 groups; physical methods, chemical methods, and biological methods. Some of the popular dye removal methods for each class were briefly explained in below.

2.4.1. Physical Methods

2.4.1.1. Adsorption

Adsorption is essentially a mass transfer phenomenon in which a substance is transferred from the liquid or gas phase to a solid surface, bound by physical or chemical interactions. The adsorption process is one of the popular methods among physical methods because it has low cost, recoverable and reusable. Parameters such as pore volume, specific surface area, adsorption capacity, and particle and pore size distribution affect dye removal performance. Generally, zeolite, alumina, silica, activated charcoal etc. are used as adsorbent (Bal and Thakur 2021). Zeolite has recently been used as a low-cost alternative in dye removal from water processes. Although the specific surface area is small, it is porous and has large molecular size. Since the diffusion limits of natural zeolites are limited, many performances improvement studies such as acid pretreatment, surfactant exchange and heat activation have been studied in the literature. One of the common materials used to remove rhodamine B dye from wastewater is Zeolite 3A. In wastewater dye mixtures, it is able to remove almost 90% of the dye adsorbent (Bal and Thakur 2021). Another adsorbent used to remove colors dispersed in water is Alumina. It is a crystalline gel and has a granular appearance. Activated carbon is a homogeneous, high surface area, microporous material that resists emissions. It is used in many industrial processes (Iqbal and Ashiq 2006). However, the disadvantages of this method are that the adsorption method is ineffective against some types of dyes and the regeneration of the adsorbent is expensive (Bal and Thakur 2021).

2.4.1.2. Coagulation/Flocculation

The coagulation/flocculation method is the separation of colloid-sized solid particles in water that cannot be precipitated by their own weight, by making them settleable with the help of various chemicals. The coagulation/flocculation method is used for the removal of parameters such as maximum chemical oxygen demand (COD), total phosphorus (TP) and total suspended solids (TSS). Coagulation of dyes has some limitations as some highly soluble low molecular weight cationic dyes may not be effectively purified, which is a disadvantage of this process. Another disadvantage is that since sludge is formed at the end of the treatment, sequential precipitation, flotation and filtration processes are applied for the removal of sludge. Generally, salts such as aluminum, iron and aluminum chloride, alum, iron (III) chloride and iron (II) sulfate are used as coagulants (Bal and Thakur 2021, Wei et al. 2018).

2.4.1.3. Membrane Filtration

Membrane technology has been widely used in industry due to its stability and high efficiency. Nanofiltration is generally the most used type among membrane filters due to its high pore size, low cost, high capacity, and ease of use (Bal and Thakur 2021). However, membrane filtration processes suffer from many important problems such as clogging of membrane surfaces resulting in reduced wastewater flow. These are the problems that increase the treatment cost. Because of the low molecular weight range of chromophoric dissolved organic compounds, it is difficult to achieve complete color removal in membrane separation processes. For these reasons, membrane filtration processes may not be suitable especially for the treatment of wastewater containing high-strength organic matter (Yoon et al. 2013).

2.4.2. Biological Methods

Biological methods are accepted as economical and environmentally friendly methods that can be used for the treatment of wastewater. The main purpose of these methods is to bring together the organic materials in the waste water and the bacteria fed with these materials and to reduce the biological oxygen requirement. Therefore, in these processes, microorganisms, bacteria, fungi, yeasts, algae, etc. required. However, these

processes are not very effective for removing dye from water because most dyestuffs are toxic to the organism and have low biodegradability (Bal and Thakur 2021).

2.4.3. Chemical Methods

2.4.3.1. Electro Fenton

The Fenton electrochemical process is a preferred and widely used method for wiping dyes from wastewater. It is mainly used to remove intense dye color and ecotoxicological effects from water. Fe^{2+} and Fe^{3+} ions are used because they produce hydroxyl radicals with oxidizing properties (Bal and Thakur 2021). This helps to remove organic pollutants. The Fenton oxidation process can be performed both homogeneously and heterogeneously under various combinations. Homogeneous Fenton oxidation may be the most extensively studied method. However, the process has two main disadvantages; The process is limited to the required acidic value ($\text{pH}=2-4$) and there is a high amount of iron ions in the solution, at the end of the reaction the iron ions must be separated from the system. This requires an additional treatment process. To overcome these problems, the metal phase is mixed with activated carbon, clay, zeolite, etc., which is called the heterogeneous Fenton process. It can be supported on a porous matrix such as (Hassan and Hameed 2011).

2.4.3.2. Ozonation

In ozonation method, some reagents can react with organic compounds. When reacting with organic pollutants, active free radicals arising from molecular ozone decomposition begin to oxidize and the wastewater loses its color. In this process, the pH value is an important criterion. The highest performance is obtained at the values where the pH value is greater than 9. The biggest advantage of ozonation is that the color can be removed without adjusting the pH in textile wastewater, without adding an extra chemical, and wastes such as residue are not formed. However, it also has disadvantages such as high capital cost, high electricity consumption, high corrosion affinity (Bal and Thakur 2021).

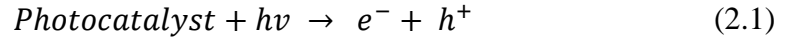
2.4.3.3. Photocatalysis

The main function of photocatalysis applications is to excite an electron from the valence band to the conduction band of the reactions. This process occurs with the help of light energy from a light source and with the formation of hydroxyl radicals. These hydroxyl radicals can attack organic structures that cause oxidation. This is because these hydroxyl radicals have a high oxidation potential. Photocatalytic processes can be applied to many different types of dyes. According to studies in the literature, the performance of dye degradation depends on various parameters such as pH, catalyst concentration, substrate concentration and the presence of electron acceptors. It has advantages such as being able to benefit from sunlight, no sludge formation, and serious reduction of COD. However, they also have problems such as contamination of catalysts and separation of catalysts from the processed liquid (Gupta 2008).

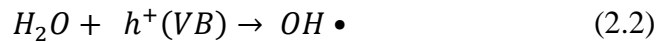
2.5. Photocatalytic Degradation

Photocatalytic degradation is the conversion of non-biodegradable dye molecules into smaller non-carcinogenic, low molecular species. This process relies on the production of highly reactive, hydroxyl and superoxide anion radicals that convert dye molecules into H₂O and CO₂. Solar energy is a resource that makes it economically feasible to treat organic pollutants with photocatalysts in photocatalytic degradation processes. Photocatalysts generally consisted of chemically stable semiconductors. These semiconductors have certain characteristics of sensitizers for photocatalytic redox reactions. In semiconductors, the band gap (E_g) separates the lowest occupied energy band (valence band, VB) from the highest vacant energy band (conductivity band, CB). The band gap energy, irradiation wavelengths and adsorption under light determine the photocatalytic activities of a semiconductor. In this way, the semiconductor with the smaller band gap shows better photocatalytic activity in the visible light region, while the semiconductor with the wider band gap shows a better photocatalytic activity in the UV region. Although catalysts have active sites for catalytic conversion, the use of the active site may not be suitable for photocatalyst use, since the reaction activity in these sites depends on the light source (Das et al. 2022).

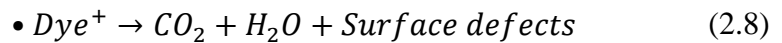
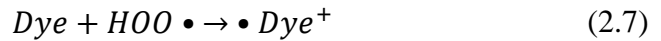
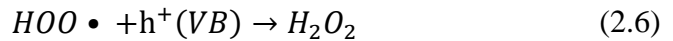
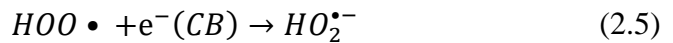
Since photocatalytic degradation makes into smaller molecules, total organic carbon valuation is an important criterion. Photocatalysis is a promising method among advanced oxidation processes due to its low cost and easy mineralization of many organic compounds. If the photon energy of a light is greater than or equal to the band gap value of the semiconductor, an electron from the valence band of the catalyst is promoted to the conduction band of the catalyst, causing electron-hole pairs to form (Das et al. 2022).



In the equation above (2.1), e^{-} indicates the electron from the conduction band and h^{+} indicates the hole from valence band. These can migrate to the surfaces of the catalyst and also undergo redox reactions with other species present on the surface. In most cases, it reacts with the surface-bound water (H_2O) molecule to form the h^{+} hydroxyl ($\bullet OH$) radicals, and with O_2 to produce the e^{-} superoxide (O_2^{-}) radical anion (Das et al. 2022).



The recombination of the excited electron and the electron hole produced in the first step is prevented by the above two steps (2.2 and 2.3). Recombination of electrons and holes takes place in the absence of oxygen. This is because oxygen captures electrons to form the superoxide radical anion (Das et al. 2022).



Schematic representation of photocatalytic degradation of RhB was shown in Figure 2.1.

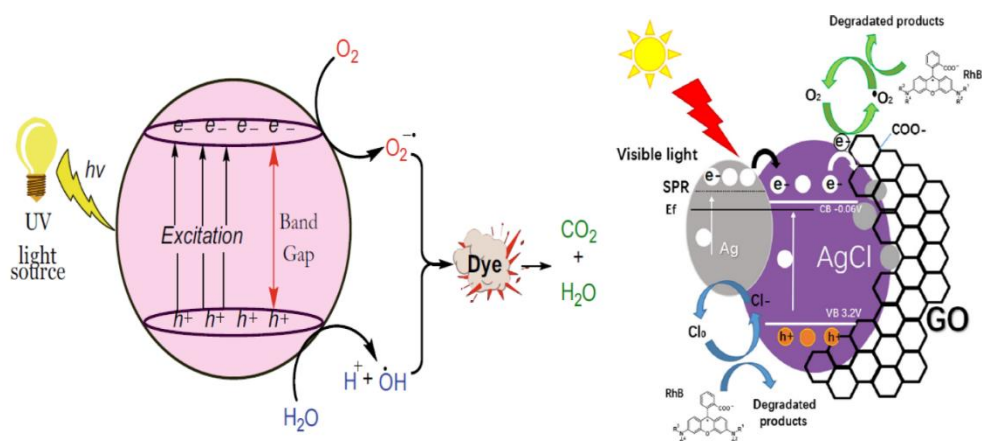


Figure 2.1. The schematic diagram of photodegradation mechanism.

The overall mechanism can be summarized as:

1. Organic pollutants are loaded onto the surface of the photocatalyst from the bulk liquid phase.
2. The pollutant is adsorbed on the active sites of the photocatalyst.
3. Superoxide anion radical ($\text{OH}\cdot$) and hydroxyl radical ($\text{O}_2^{\bullet-}$) degrade pollutants.
4. The final product is separated from the surface of the catalyst.
5. The bulk of the remaining product is transferred to the bulk liquid phase.

CHAPTER 3

MATERIALS AND METHODS

3.1. Materials

Rhodamine B dye was purchased from Merck. Silver nitrate (AgNO_3) purchased from Carlo Erba. Ethylene glycol ($\text{C}_2\text{H}_6\text{O}_2$), sodium chloride (NaCl), and Graphene Oxide (GO), HCl were supplied from VWR Chemicals, and Aldrich respectively. For the washing steps, ethanol was purchased from Tekkim.

3.2. Synthesis of Photocatalysts

3.2.1. Synthesis of Ag/AgCl and Ag/AgCl@GO Catalysts

To synthesize Ag/AgCl@GO photocatalyst, 1.59 mmol of AgNO_3 was dissolved in 10 mL of deionized water and 30 mL of ethylene glycol mixture. At the same time, 5 mL of (2 mg/mL) GO-water mixture was prepared and added to the mixed solution dropwise while it is stirring for 1h. After that, 5 mL of KCl solution (0.350 mol/L) was added to the mixture dropwise and keep continuing to stir for 3h. The obtained mixture was centrifuged at 7000 rpm for 5 min. The obtained precipitate was washed two times with ethanol and two times with deionized water respectively at 7000 rpm for 5 min. 50 mL of deionized water was added to the washed product and stirred at a UV lamp for 10 min. Then it is centrifuged at 7000 rpm for 5 min. Finally, the product was obtained by drying the precipitate at 70°C for 24h (Figure 3.1) (Ai 2019).

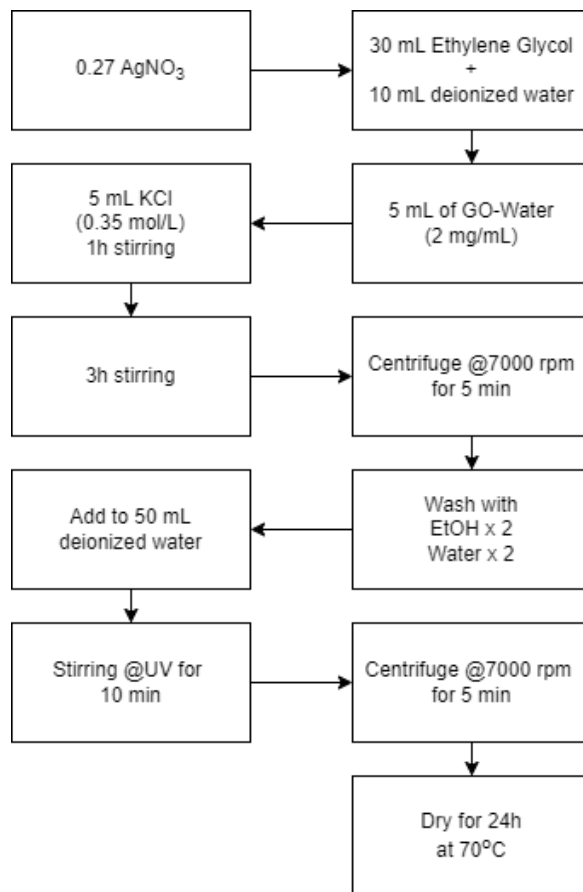


Figure 3.1 Synthesis diagram of Ag/AgCl@GO photocatalyst.



Figure 3.2 Silver nitrate solution (a), Solution with added GO (b), Solution after adding KCl (c,d), Final product Ag/AgCl@GO (e).

The same procedure was applied to synthesize Ag/AgCl photocatalyst. However, instead of GO solution, 5 mL of deionized water was used. Schematic representation of the synthesized was illustrated in Figure 3.3 and obtained product shown in Figure 3.4 (Ai 2019).

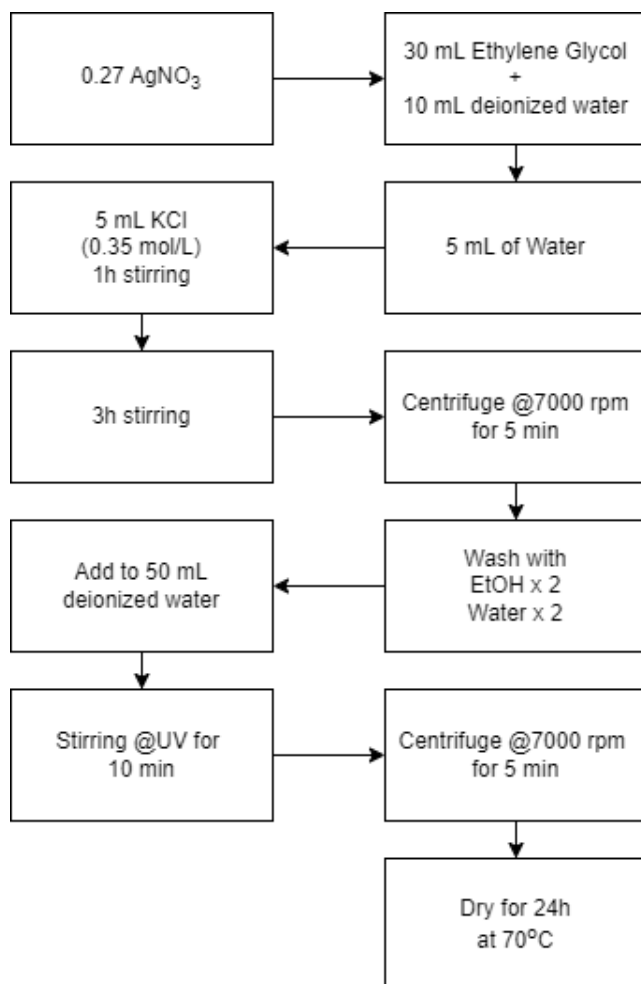


Figure 3.3. Synthesis diagram of Ag/AgCl photocatalyst.

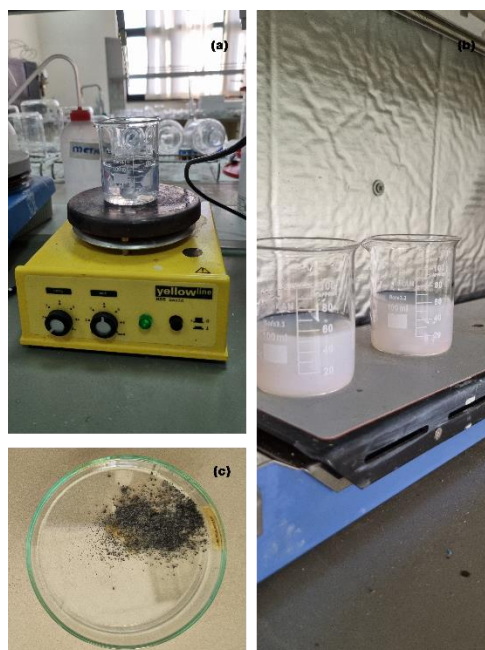


Figure 3.4. Silver nitrate solution (a), Solution after adding KCl (b), Final product Ag/AgCl (c).

3.2.2. Synthesis of UiO-66-NH₂

Figure 3.5. shows that the synthesis diagram of the synthesized MOF. Briefly, 0.0811 g of zirconium chloride and 0.0471 g of 2 aminoterephthalate acid were sonicated in 60 mL of DMF. It was then heated at 120 degrees for 24 hours. After spontaneous cooling to room temperature, it was centrifuged and washed 3 times with DMF and 3 times with methanol. The resulting product was finally dried at 60 degrees under vacuum for 12 hours (Zhao et al 2019).

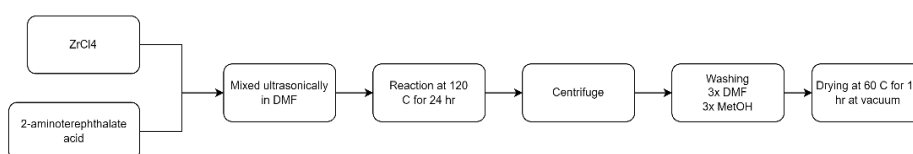


Figure 3.5. Synthesis diagram of UiO-66-NH₂.

3.2.3. Synthesis of UiO-66-NH₂-Ag/AgCl

Figure 3.6. shows the synthesis diagram of synthesized MOF photocatalyst. 0.2 g of synthesized UiO-66-NH₂ was dissolved in 100 mL of deionized water. It was sonicated for 30 min. Then, 0.1 mol/L AgNO₃ solution was dropped into the suspension with mechanical mixing. This mixture was stirred for 10 minutes and then sonicated for 20

minutes. After that, 0.1 mol/L HCl solution was added to the mixture. After 10 minutes of mixing in the dark, the resulting mixture was stirred for another 30 minutes under UV light. Thanks to this mixing, Ag⁺ was reduced to Ag⁰. The obtained sample was centrifuged and washed 3 times with deionized water. Then, finally, it was dried by vacuuming at 60 degrees for 12 hours (Zhao et al 2019).

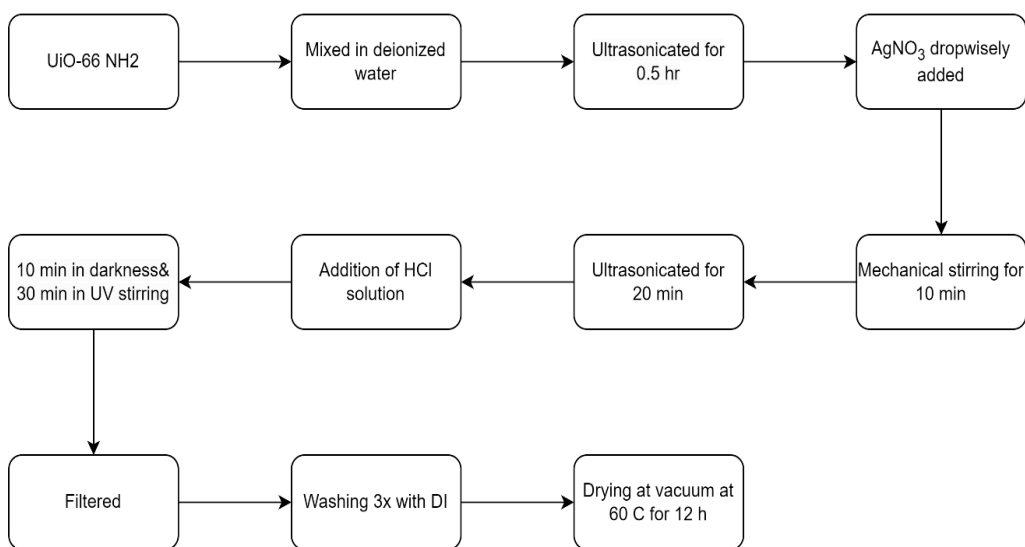


Figure 3.6. Synthesis diagram of UiO-66-NH₂-Ag/AgCl.

3.3. Characterization Studies

The photocatalysis (Ag/AgCl, Ag/AgCl@GO) was characterized with X-Ray diffraction (XRD), scanning electron microscope (SEM).

X-Ray diffraction (XRD) was used to determine the crystalline structure. Phillips X'Pert diffractometer was used at scan mode of 0.04°/s with CuK α radiation. The 2 θ angle is between 5° to 90°.

The surface morphology of synthesized Ag/AgCl, UiO-66-NH₂-Ag/AgCl and Ag/AgCl@Go were analyzed via SEM analysis with FEI QUANTA 250 FEG model device.

After photocatalytic analysis UV-Vis spectrometer (Shimadzu UV-2000) was used to determine the optical properties of photocatalysts.

3.4. Photocatalytic Experiments

The photocatalytic experiments were performed to evaluate the photocatalytic degradation of RhB in deionized water under visible light irradiation. The chemical structure of RhB was shown in Figure 3.7. In the mechanism, fluorescence dye has a non-specific attachment to a substrate.

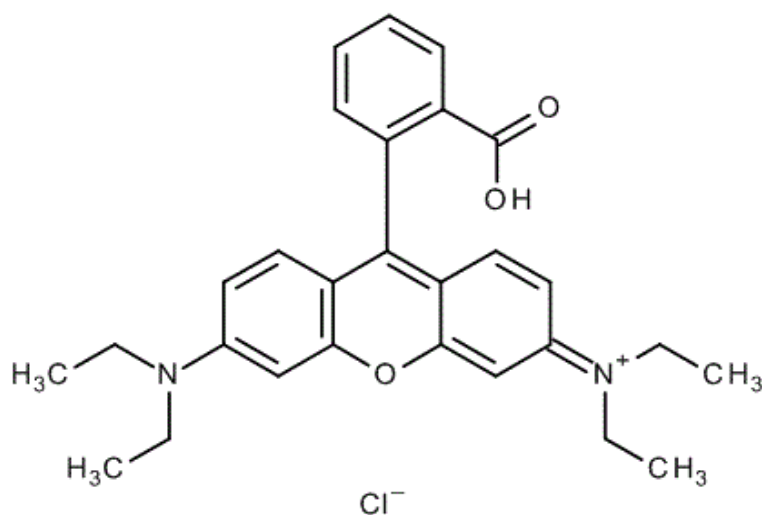


Figure 3.7. Chemical structure of rhodamine B dye (Source: Alé et al. 2020).

The photocatalytic degradation process was performed on a closed experimental setup (Figure 3.8). There is an OSRAM HNS 15W G13 Hg fluorescence lamp was used.



Figure 3.8. Experimental setup.

In the reaction, 10 ppm of RhB solution and 40 mg of catalyst was magnetically stirred for 15 min in dark condition. After that, at every 15 minutes, 2 mL samples were taken to analyze in presence of a light source while samples were magnetically stirred. All the collected samples were filtered to remove catalysts from the dye for determining the dye concentration. Then UV-Vis. spectroscopy was used to perform analyses at 554 nm which is determined from Figure 3.9. as the peak value.

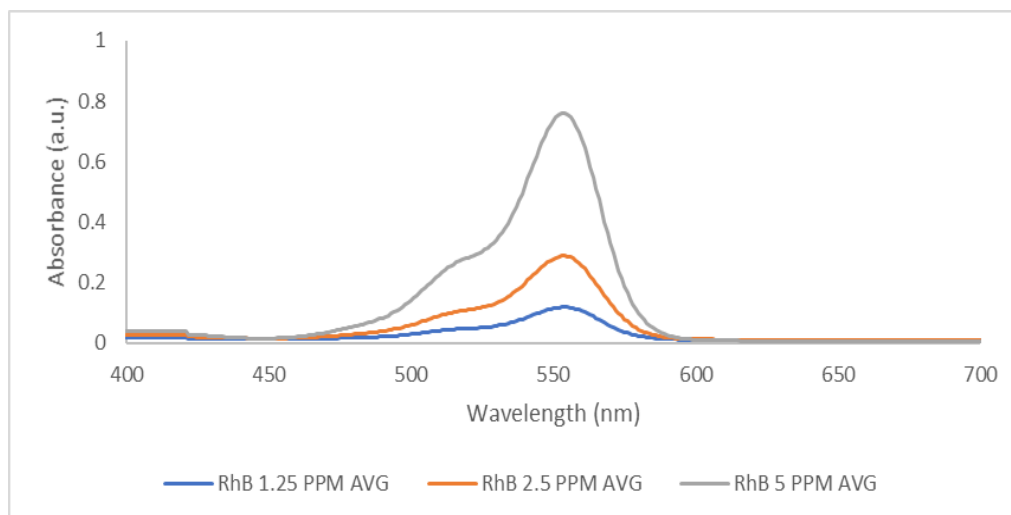


Figure 3.9. The emission spectra of RhB in different concentrations.

The effect of pH on photocatalytic degradation performance was also considered. Therefore 3 different pH values were tried on photocatalysts which are pH 3, pH 8 (neutral), pH 11 for Ag/AgCl and pH 3, pH 8 (neutral), and pH 11 for Ag/AgCl@GO and pH 3, pH 8 (neutral), pH 11 for UiO-66-NH₂-Ag/AgCl. To reduce the pH value of HCl, to increase the pH value NaOH was used. All pH measurements were determined with the Sartorius Docu-ph⁺ meter model.

CHAPTER 4

RESULTS AND DISCUSSION

4.1. Characterization Results of Ag/AgCl and Ag/AgCl@GO Photocatalysts

4.1.1. XRD Analysis

Figure 4.1 shows the XRD pattern of synthesized photocatalysts. AgCl crystals of synthesized photocatalysts correspond to (1 1 1), (2 0 0), (2 2 0), (3 1 1), (2 2 2), (4 0 0) planes respectively 27.8, 32.3, 46.3, 54.9, 57.5, 67.5, 74.5, 76.8 diffraction peaks were observed. It has been proven by the (3 3 1) and (4 2 0) crystal planes that GO addition has no effect on the formation of AgCl crystals during the synthesis process. Due to the low Ag^0 content of the Ag element in the material, the diffraction peak could not be visualized.

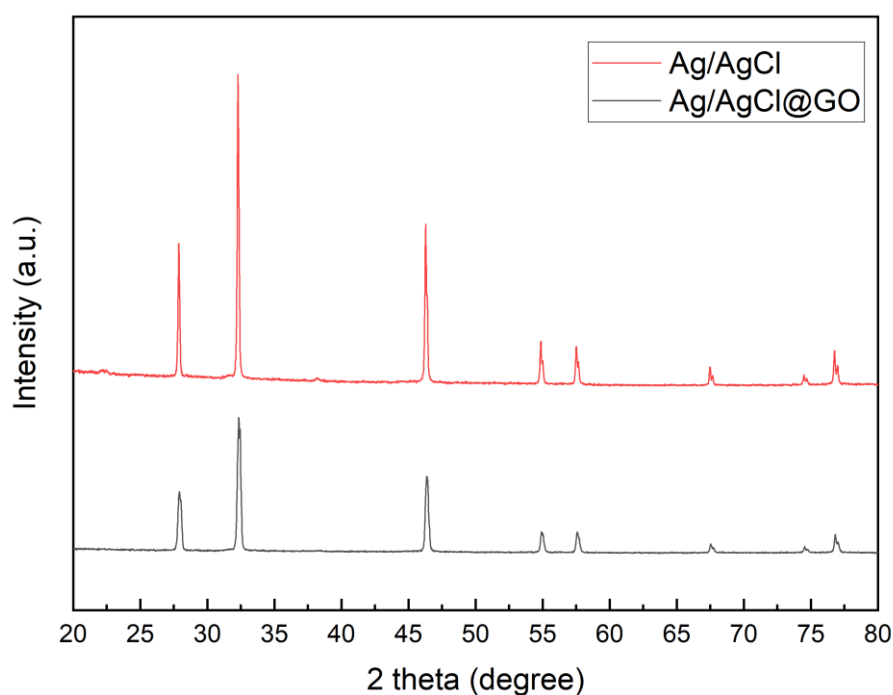


Figure 4.1. XRD of Ag/AgCl@GO and Ag/AgCl.

4.1.2. SEM Analysis

Figure 4.2. shows the SEM images and particle size distribution graph of each photocatalyst. Particle size of each photocatalysts were calculated with “ImageJ software”. After finding the particle sizes (L), amount of these particles sizes vs particle size graphed were drawn. Average particle diameter of each photocatalyst was found as 2 μm , 3.25 μm and 0.225 μm for Ag/AgCl@GO, Ag/AgCl and UiO-66-NH₂-Ag/AgCl respectively from the Figure 4.2. It can also say that for Ag/AgCl@GO particles are agglomerated.

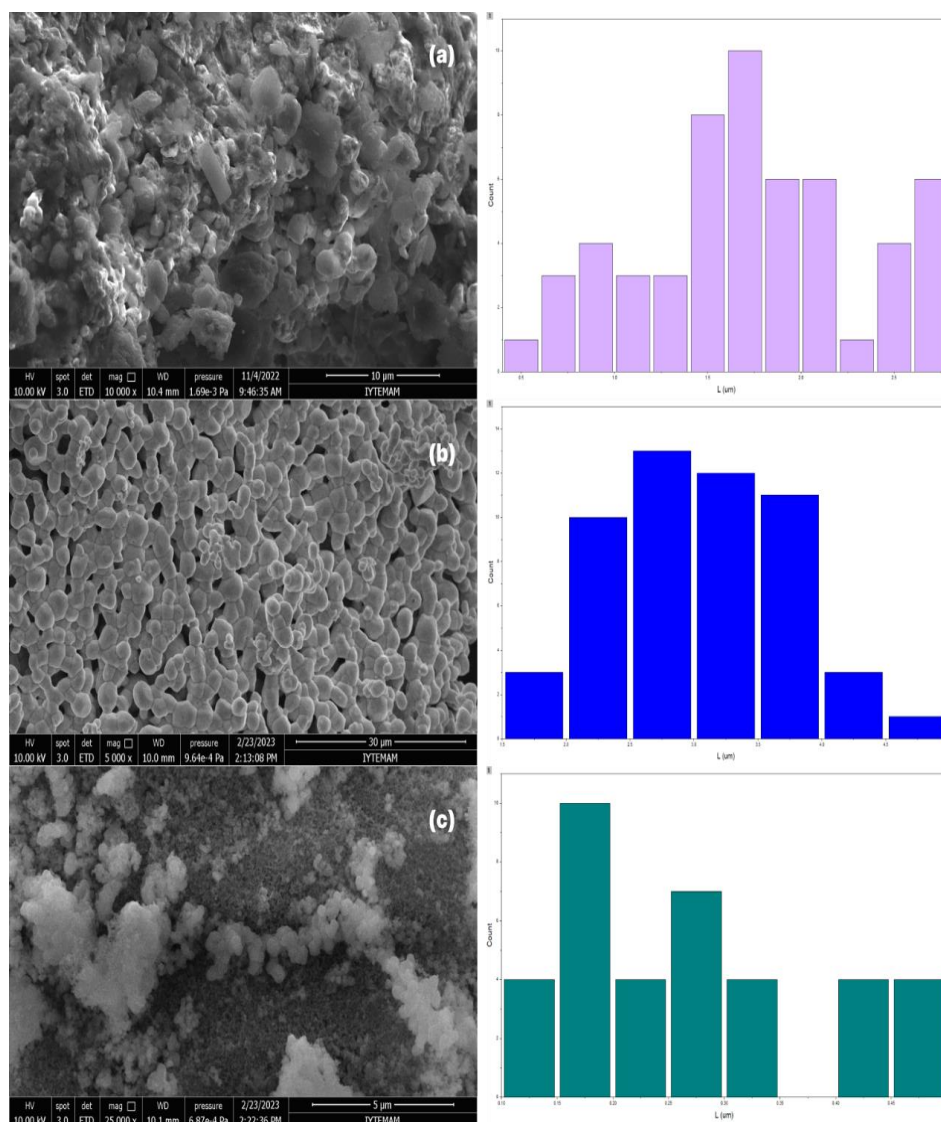


Figure 4.2. SEM images and particle size graphs of Ag/AgCl@GO (a), Ag/AgCl (b), UiO-66-NH₂-Ag/AgCl (c).

4.1.3. TGA Analysis

Figure 4.3 (a) and (b) shows similar downward trend. For both figure, there is no weight loss until 700 °C. Ag/AgCl and Ag/AgCl@GO showed excellent thermal stability. Figure 4.3 (c) shows that synthesized photocatalyst between 30°C and 200°C UiO-66-NH₂ is losing weight due to volatilization of residual organics such as solvents in the pores. After that the weight loss between 200 °C and 900°C is because of the collapse of the framework structure which is supplemented by formed oxides. Between 120 °C and 700 °C, UiO-66-NH₂ loses weight with the support of the collapse of the framework structure and oxide formation. After 700 °C, the main reason for the weight loss is the formation of completed oxides due to the collapse of the frame structure. When the weight loss of the sample no longer changed, the framework structure of UiO-66-NH₂ completely collapsed and the samples were all zirconium oxide.

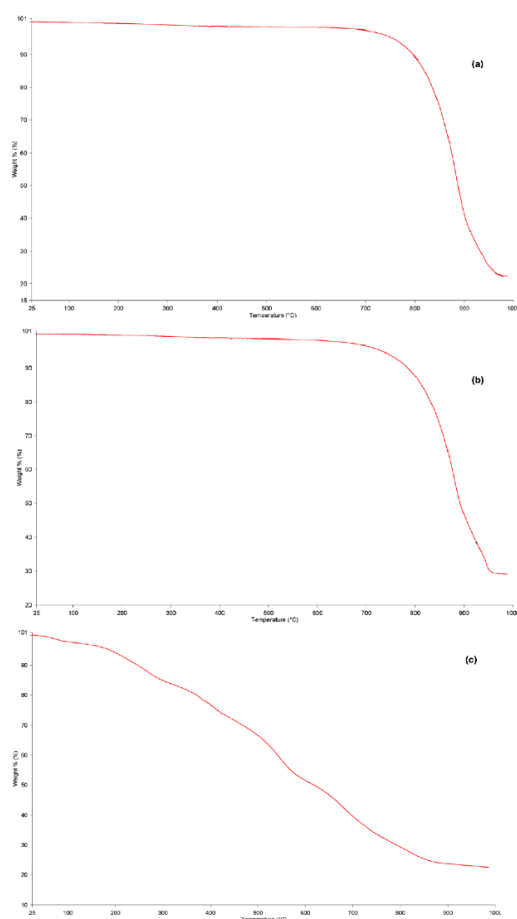


Figure 4.3. TGA results of Ag/AgCl (a), Ag/AgCl@GO (b), and UiO-66-NH₂-Ag/AgCl (c).

4.2. Photocatalytic Degradation Results of RhB

4.2.1. Effect of pH

Experiments were carried out at pH: 3, pH: 8 (natural pH value of the solutions), pH: 11 by using 30 mg of photocatalyst in 50 ml dye solution at 10 ppm concentration of rhodamine B dyestuff with Ag/AgCl based photocatalysts. First 15 minutes of the experiment was performed in the dark conditions. After that photocatalytic degradation started with UV condition. After introducing the UV light to the sample's degradation started and removal of the dye was observed remarkably. It is observed that the degradation of RhB and the subsequent reduction is delayed due to the high concentration of protons. As a result of the experiments, the effect of pH value on the photocatalytic removal of Rhodamine B dye was observed. The best performances were observed for all photocatalysts at pH: 8, that is, at its natural value. The graph of Rhodamine B dye concentration changing according to pH value in 90 minutes is given in the Figure 4.3.

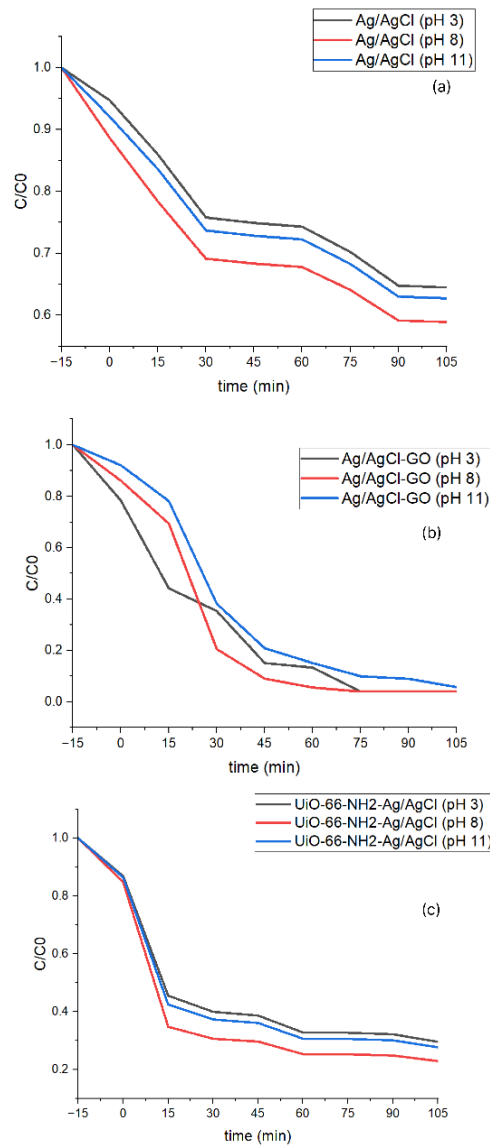


Figure 4.4 Concentration change for different pH values with time.

According to the results in Figure 4.4, studies were continued with natural pH values.

4.2.2. Rhodamine B Removal in Different Catalyst Weights

To find the optimum Ag/AgCl, UiO-66-NH₂-Ag/AgCl and Ag/AgCl@GO photocatalyst content, the results of the removal performances of different amounts of photocatalysts (10 mg to 50 mg) in 10 ppm Rhodamine B dye solution are shown in Figure 4.5. According to the results, there were no visible changes in the removal performance after 40 mg. Catalyst content with 40 mg, 52%, 87%, 96% of RhB removed for Ag/AgCl, UiO-66-NH₂-Ag/AgCl and Ag/AgCl@GO respectively.

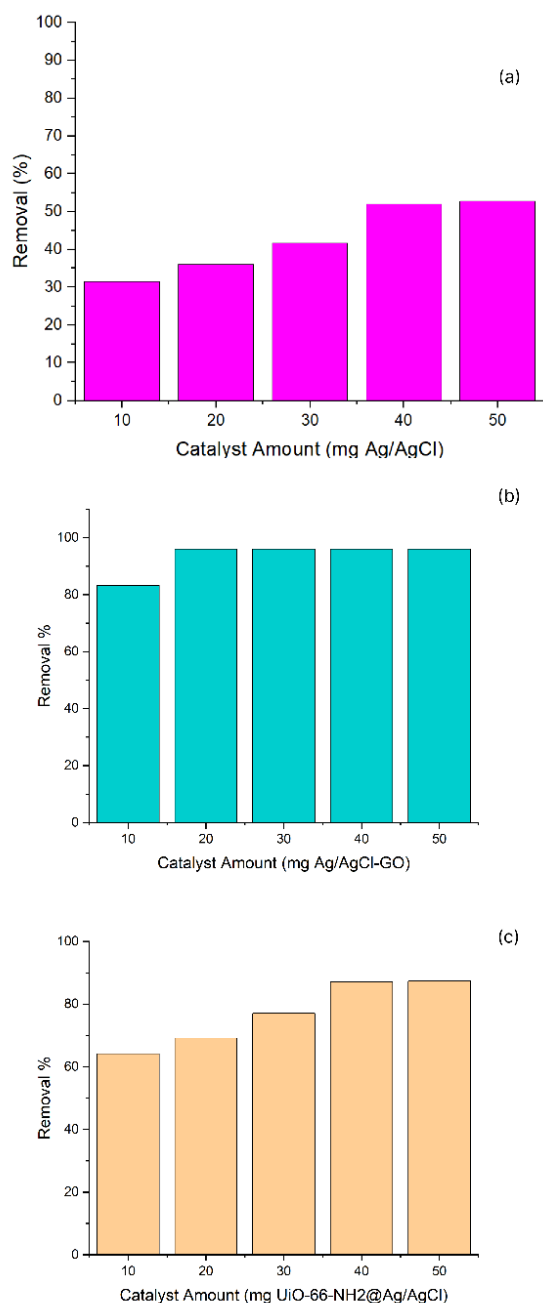


Figure 4.5. Photocatalytic degradation performance of each photocatalysts for different catalyst amounts (at their neutral pH (8) values).

The removal of Ag/AgCl, UiO-66-NH₂-Ag/AgCl and Ag/AgCl@GO photocatalysts for 10 ppm Rhodamine B dye in 90 minutes was followed. The first 15 minutes of the studies were in the dark, and the 90 minutes were done under UV light. The concentration graph of the experiment performed is shown in Figure 4.6.

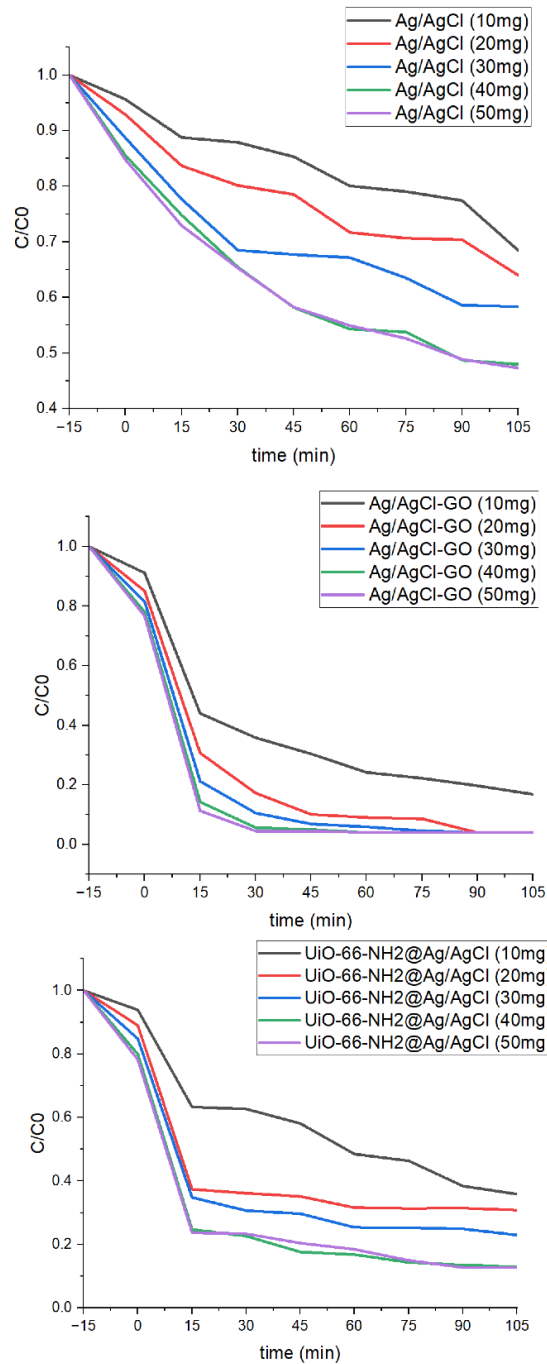


Figure 4.6. Concentration changes with time of each photocatalysts for different catalyst amounts (at their neutral pH values).

4.2.3. Rhodamine B Removal in Different Dye Amount

In order to observe the effect of the initial dye concentration on the dye removal performance, dye solutions between 10 ppm and 40 ppm were used. The degradation performance of Rhodamine B depends on the amount of dye as seen in Figure 4.7.

Especially in Ag/AgCl and UiO-66-NH₂-Ag/AgCl photocatalysts, the removal visibly changes according to the amount of dye.

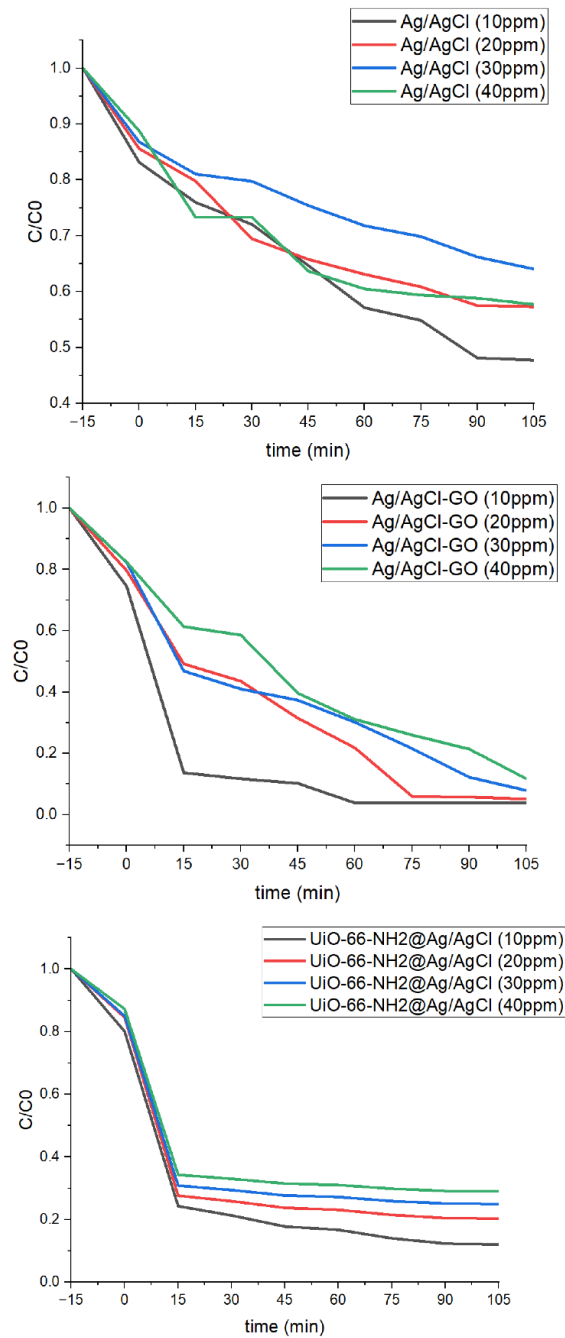


Figure 4.7. Photocatalytic degradation performance of photocatalysts with different dye amount.

4.2.4. Rhodamine B Removal Comparison

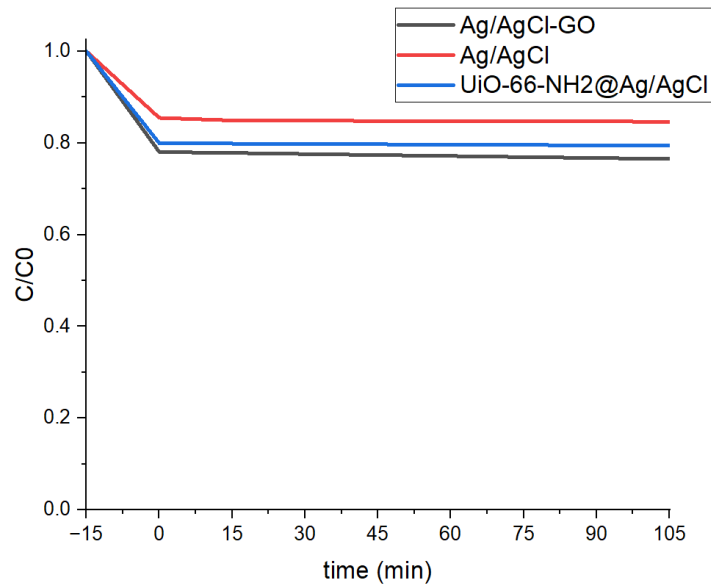


Figure 4.8. RhB photodegradation without light.

Figure 4.8. shows that degradation of all photocatalyst in the absence of UV-light is so less. Therefore, this process is not adsorption-driven. The light removal results of Ag/AgCl, UiO-66-NH₂-Ag/AgCl, Ag/AgCl@GO and bare rhodamine B were compared in Figure 4.7.

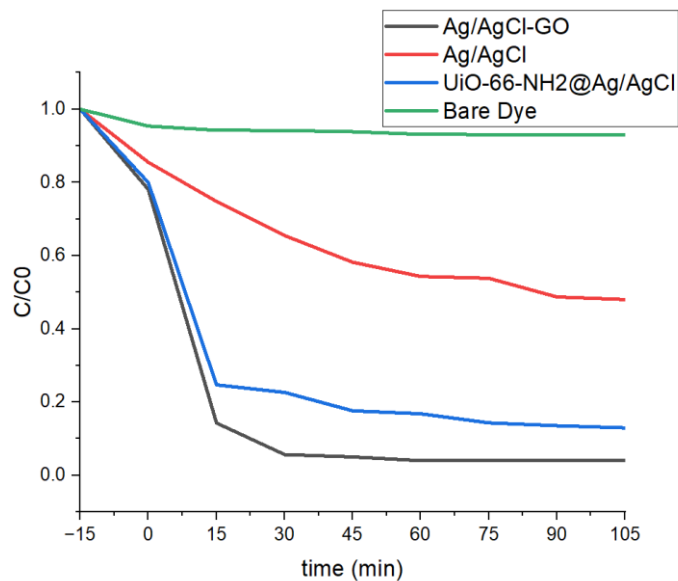


Figure 4.9. Comparison of concentration change of each samples with time.

After 90 minutes of UV irradiation, the remaining dye content ratio is 48%, 4% and 93%, 13% in Ag/AgCl, Ag/AgCl@GO, bare dye and, UiO-66-NH₂-Ag/AgCl respectively. Ag/AgCl@GO is the catalyst with the best removal performance. It may be because of the increase in the response of the composite to visible light which might increase photocatalytic activity in Ag⁰ particles formed in the Ag/AgCl-GO photocatalysis. Increasing the specific area of the catalyst which is good for the adsorption contact of dye with catalyst. This situation may be occurred with addition of GO. In addition, an electron migration may have occurred in the photocatalyst, which delays the recombination of photogenerated carriers with presence of GO (Ai et al. 2019, Chen et al. 2013, Ahmed et al. 2016, Miao et al. 2017).

4.2.5. Photoluminescence Spectra (PL) Results of Photocatalysts

To calculate the band gap energy, equation 4.1. was used.

$$E = hv = \frac{hc}{\lambda} \quad (4.1)$$

Where h is Planck's constant, v is frequency, c is the speed of light and λ is wavelength. Since Planck's constant is 6.626×10^{-34} m²kg/s and speed of light is $2,99 \times 10^8$. Equation becomes:

$$E = \frac{12,400}{\lambda} \quad (4.2)$$

Table 4.1. shows the band gap and PL excitation wavelengths of all photocatalysts. There are two peaks in each photocatalytic powder. One of these peaks are from UV-region, and the other peaks are from visible region. Results showed that any addition to Ag/AgCl slightly shifted to visible region. With addition of GO didn't change the wavelength. It might be because of the agglomeration that have seen in SEM images. The MOF structure with Ag/AgCl, wavelength become shifted more to the visible region and which has lower band gap and energy.

Table 4.1. PL results of samples.

Samples	UV Region		Visible Region	
	Band Gap (eV)	Wavelength (nm)	Band Gap (eV)	Wavelength (nm)
Ag/AgCl	4.20	295	2.95	420
Ag/AgCl@GO	4.18	297	2.96	419
UiO-66-NH ₂ -Ag/AgCl	4.18	297	2.70	460

4.2.6. Kinetics

In order to examine the reaction kinetics, a kinetic plot was calculated using a pseudo-first-order-model for 10 ppm RhB and 40 mg catalyst amount for every photocatalyst. The equation used in this model is given below:

$$\ln(C_0/C) = kt \quad (4.3)$$

where C_0 original concentration of RhB (mg/L), C concentration of RhB at a time (mg/L), k is the reaction rate constant (min^{-1}) and t is the time (min).

The slope of the $\ln(C_0/C)$ graph gives the reaction constant k in the first-order kinetic. According to Figure 4.10, the reaction constants for Ag/AgCl, Ag/AgCl@GO and UiO-66-NH₂-Ag/AgCl were found to be 0.0061 min^{-1} , 0.0274 min^{-1} and 0.0166 min^{-1} , respectively. Ag/AgCl@GO has the highest reaction rate value. This value is 1.7 times higher than UiO-66-NH₂-Ag/AgCl and 4.5 times higher than Ag/AgCl.

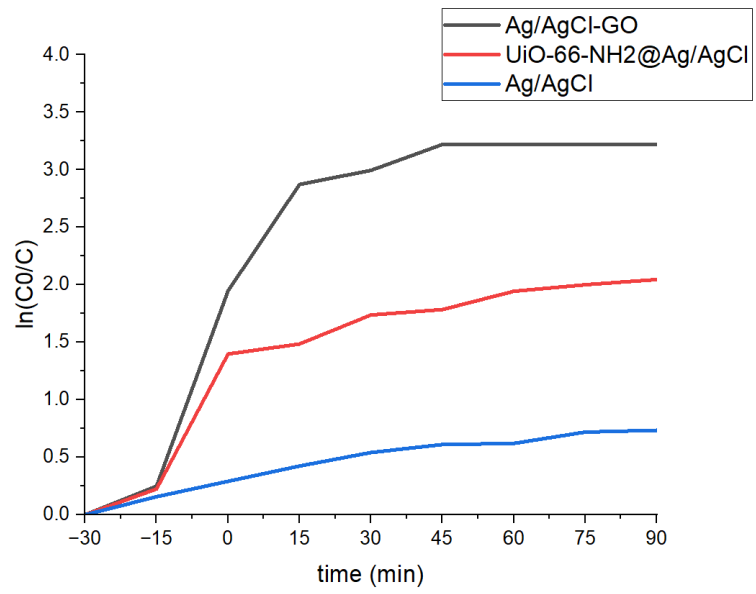


Figure 4.10. Kinetic data of photocatalysts with pseudo-first-order- model.

CHAPTER 5

CONCLUSION

In this study, Ag/AgCl, UiO-66-NH₂-Ag/AgCl and Ag/AgCl@GO photocatalysts were synthesized for the removal of rhodamine b dyestuff in wastewater by photocatalytic removal and some of the parameters affecting the removal performance were investigated.

In this study, firstly, the synthesis of Ag/AgCl, UiO-66-NH₂-Ag/AgCl and Ag/AgCl@GO photocatalysts was successfully performed. Some characterization studies such as XRD, SEM and PL spectra have been carried out.

Then, experiments were carried out in natural pH environment and under visible light to examine the photocatalytic performance of photocatalysts. At the same time, the effect of pH amount on photocatalytic performance was investigated and natural pH environment proved to be the most efficient. In addition, the performance of different amounts of photocatalyst in 10 ppm paint was investigated. According to the results, there is no change in photocatalytic performance after 40 mg. Therefore, the optimum amount of catalyst was determined as 40 mg. In addition, studies were carried out with different amounts of dye and it was observed that the photocatalytic performance decreased with the use of a 40 mg catalyst as the dye concentration increased. Finally, a comparison of bare dye, Ag/AgCl, UiO-66-NH₂-Ag/AgCl and Ag/AgCl@GO photocatalysts was made and it was observed that Ag/AgCl@GO material had the highest dye removal performance. Based on this result, it was observed that the addition of GO increased the photocatalytic performance and dye removal. After that PL spectra of each photocatalysts were taken and results showed that addition to Ag/AgCl powder does not change wavelength remarkably.

Ag/AgCl@GO catalyst produced in future studies may also work for the removal of other dyes. Combination of other MOFs with Ag/AgCl can also be investigated. In addition, a more cost-effective photocatalyst study can be done by combining Ag/AgCl material with other materials.

REFERENCES

- Ahmed, Gulzar, Muddasir Hanif, Lizhong Zhao, Mozaffar Hussain, Javid Khan, and Zhongwu Liu. "Defect Engineering of ZnO Nanoparticles by Graphene Oxide Leading to Enhanced Visible Light Photocatalysis." *Journal of Molecular Catalysis A: Chemical* 425 (2016): 310–21.
- Ai, Cuiling, Sikai Yang, Fan Zhang, Xiangwen Shao, and Junge Xu. "AG/AGCL-Go: A Composite for Degradation of Rhodamine B in Dye Wastewater." *Advanced Powder Technology* 30, no. 12 (2019): 3193–3202.
- Ajmal, Anila, Imran Majeed, Riffat Naseem Malik, Hicham Idriss, and Muhammad Amtiaz Nadeem. "Principles and Mechanisms of Photocatalytic Dye Degradation on TiO₂Based Photocatalysts: A Comparative Overview." *RSC Adv.* 4, no. 70 (2014): 37003–26.
- Al-Gheethi, Adel Ali, Qasdina Marsya Azhar, Ponnusamy Senthil Kumar, Abdiadim Abdirizak Yusuf, Abdullah Khaled Al-Buriah, Radin Maya Radin Mohamed, and Muhanna Mohammed Al-shaibani. "Sustainable Approaches for Removing Rhodamine B Dye Using Agricultural Waste Adsorbents: A Review." *Chemosphere* 287 (2022): 132080.
- Allé, Paul Henri, Guy Didier Fanou, Didier Robert, Kopoin Adouby, and Patrick Drogui. "Photocatalytic Degradation of Rhodamine B Dye with TiO₂ Immobilized on SIC Foam Using Full Factorial Design." *Applied Water Science* 10, no. 9 (2020).
- Bal, Gurleen, and Archana Thakur. "Distinct Approaches of Removal of Dyes from Wastewater: A Review." *Materials Today: Proceedings* 50 (2022): 1575–79.
- Bhat, Sajad Ahmad, Nusrat Rashid, Mudasir Ahmad Rather, Sarwar Ahmad Bhat, Pravin P. Ingole, and Mohsin Ahmad Bhat. "Highly Efficient Catalytic Reductive Degradation of Rhodamine-B over Palladium-Reduced Graphene Oxide Nanocomposite." *Chemical Physics Letters* 754 (2020): 137724.
- Chen, Guodong, Meng Sun, Qin Wei, Yongfang Zhang, Baocun Zhu, and Bin Du. "AG₃PO₄/Graphene-Oxide Composite with Remarkably Enhanced Visible-Light-

- Driven Photocatalytic Activity toward Dyes in Water.” *Journal of Hazardous Materials* 244-245 (2013): 86–93.
- Chowdhury, Pankaj, Sharmistha Nag, and Ajay K. Ray. “Degradation of Phenolic Compounds through UV and Visible- Light-Driven Photocatalysis: Technical and Economic Aspects.” *Phenolic Compounds - Natural Sources, Importance and Applications*, 2017. <https://doi.org/10.5772/66134>.
- Das, Bubul, Hirendra Nath Dhara, Anjali Dahiya, and Bhisma K. Patel. “Recent Advances in Photocatalytic Degradation of Dyes Using Heterogeneous Catalysts.” *Trends and Contemporary Technologies for Photocatalytic Degradation of Dyes*, 2022, 21–64.
- Dutta, Soumi, Bramha Gupta, suneel Kumar srivastava, and Ashok Kumar Gupta. “Recent Advances on the Removal of Dyes from Wastewater Using Various Adsorbents: A Critical Review.” *Materials Advances*, 2021.
- “Dyeing with Coal Tar Dyestuffs. by C. M. Whittaker. Pp. x + 214. (London: Bailliere, Tindall and Cox, 1918.) Price 7s. 6d. Net.” *Journal of the Society of Chemical Industry* 38, no. 2 (1919): 35–36.
- “Dyes, General Survey.” *Industrial Dyes*, n.d., 1–12.
- Elvers, Barbara. *Ullmann's Encyclopedia of Industrial Chemistry*. Weinheim: VCH, 1993.
- Gupta, V.K., and Suhas. “Application of Low-Cost Adsorbents for Dye Removal – a Review.” *Journal of Environmental Management* 90, no. 8 (2009): 2313–42.
- Gürses Ahmet, Açıkyıldız Metin, Güneş Kübra, and Gürses M. Sadi. *Dyes and Pigments*. Switzerland: Springer, 2016.
- Hassan, H., and B.H. Hameed. “Fenton-like Oxidation of Acid Red 1 Solutions Using Heterogeneous Catalyst Based on Ball Clay.” *International Journal of Environmental Science and Development*, 2011, 218–22.
- Hunger, Klaus. *Industrial Dyes*. Weinheim: Wiley-Blackwell, 2003.

- Imam, Saifullahi Shehu, and Halimah Funmilayo Babamale. "A Short Review on the Removal of Rhodamine B Dye Using Agricultural Waste-Based Adsorbents." *Asian Journal of Chemical Sciences*, 2020, 25–37.
- Kant, Rita. "Textile Dyeing Industry an Environmental Hazard." *Natural Science* 04, no. 01 (2012): 22–26.
- Maheshwari, Karishma, Madhu Agrawal, and A. B. Gupta. "Dye Pollution in Water and Wastewater." *Sustainable Textiles: Production, Processing, Manufacturing & Chemistry*, 2021, 1–25.
- Miao, Xuli, Xiaoping Shen, Jiajia Wu, Zhenyuan Ji, Jiheng Wang, Lirong Kong, Miaomiao Liu, and Chunsen Song. "Fabrication of an All Solid Z-Scheme Photocatalyst G-C 3 N 4 /Go/AgBr with Enhanced Visible Light Photocatalytic Activity." *Applied Catalysis A: General* 539 (2017): 104–13.
- Piaskowski, Krzysztof, Renata Świdorska-Dąbrowska, and Paweł K Zarzycki. "Dye Removal from Water and Wastewater Using Various Physical, Chemical, and Biological Processes." *Journal of AOAC INTERNATIONAL* 101, no. 5 (2018): 1371–84.
- R Ananthashankar, AE Ghaly. "Production, Characterization and Treatment of Textile Effluents: A Critical Review." *Journal of Chemical Engineering & Process Technology* 05, no. 01 (2013).
- Rafiq, Asma, Muhammad Ikram, S. Ali, Faiza Niaz, Maaz Khan, Qasim Khan, and Muhammad Maqbool. "Photocatalytic Degradation of Dyes Using Semiconductor Photocatalysts to Clean Industrial Water Pollution." *Journal of Industrial and Engineering Chemistry* 97 (2021): 111–28.
- Rashid, Tazien, Danish Iqbal, Abu Hazafa, Sadiq Hussain, Falak Sher, and Farooq Sher. "Formulation of Zeolite Supported Nano-Metallic Catalyst and Applications in Textile Effluent Treatment." *Journal of Environmental Chemical Engineering* 8, no. 4 (2020): 104023.
- Samsami, Shakiba, Maryam Mohamadizani, Mohammad-Hossein Sarrafzadeh, Eldon R. Rene, and Meysam Firoozbahr. "Recent Advances in the Treatment of Dye-Containing

- Wastewater from Textile Industries: Overview and Perspectives.” *Process Safety and Environmental Protection* 143 (2020): 138–63.
- Shahid, Mohammad, Julie Wertz, Ilaria Degano, Maurizio Aceto, Mohd Ibrahim Khan, and Anita Quye. “Analytical Methods for Determination of Anthraquinone Dyes in Historical Textiles: A Review.” *Analytica Chimica Acta* 1083 (2019): 58–87.
- Slama, Houada Ben, Ali Chenari Bouket, Zeinab Pourhassan, Faizah N. Alenezi, Allaoua Silini, Hafsa Cherif-Silini, Tomasz Oszako, Lenka Luptakova, Patrycja Golińska, and Lassaad Belbahri. “Diversity of Synthetic Dyes from Textile Industries, Discharge Impacts and Treatment Methods.” *Applied Sciences* 11, no. 14 (2021): 6255.
- Sundararajan, M., V. Sailaja, L. John Kennedy, and J. Judith Vijaya. “Photocatalytic Degradation of Rhodamine B under Visible Light Using Nanostructured Zinc Doped Cobalt Ferrite: Kinetics and Mechanism.” *Ceramics International* 43, no. 1 (2017): 540–48.
- Viswanathan, B. “Photocatalytic Degradation of Dyes: An Overview.” *Current Catalysis* 7, no. 2 (2018): 99–121.
- Wei, Hua, Boqiang Gao, Jie Ren, Aimin Li, and Hu Yang. “Coagulation/Flocculation in Dewatering of Sludge: A Review.” *Water Research* 143 (2018): 608–31.
- Yoon, Yeojoon, Yunyoung Hwang, Minhwan Kwon, Youmi Jung, Tae-Mun Hwang, and Joon-Wun Kang. “Application of O₃ and O₃/H₂O₂ as Post-Treatment Processes for Color Removal in Swine Wastewater from a Membrane Filtration System.” *Journal of Industrial and Engineering Chemistry* 20, no. 5 (2014): 2801–5.
- Zhang, Lian, Qianqian Shao, and Chunhua Xu. “Enhanced Azo Dye Removal from Wastewater by Coupling Sulfidated Zero-Valent Iron with a Chelator.” *Journal of Cleaner Production* 213 (2019): 753–61.
- Zhao, Wanyue, Tong Ding, Yating Wang, Moqing Wu, Wenfeng Jin, Ye Tian, and Xingang Li. “Decorating AG/AGCL on UIO-66-NH₂: Synergy between Ag Plasmons and Heterostructure for the Realization of Efficient Visible Light Photocatalysis.” *Chinese*

Journal of Catalysis 40, no. 8 (2019): 1187–97. [https://doi.org/10.1016/s1872-2067\(19\)63377-2](https://doi.org/10.1016/s1872-2067(19)63377-2).

Zou, D., and D. Liu. “Understanding the Modifications and Applications of Highly Stable Porous Frameworks via UIO-66.” *Materials Today Chemistry* 12 (2019): 139–65. <https://doi.org/10.1016/j.mtchem.2018.12.004>.